

Scalar vacuum densities on Beltrami pseudosphere

T. A. Petrosyan*

*Institute of Physics, Yerevan State University,
1 Alex Manoogian Street, 0025 Yerevan, Armenia*

January 8, 2026

Abstract

We investigate the combined effects of spatial curvature and topology on the properties of the vacuum state for a charged scalar field localized on the (2+1)-dimensional Beltrami pseudosphere, assuming that the field obeys quasiperiodicity condition with constant phase. As important local characteristics of the vacuum state the vacuum expectation values (VEVs) of the field squared and energy-momentum tensor are evaluated. The contributions in the VEVs coming from geometry with an uncompactified azimuthal coordinate are divergent, whereas the compact counterparts are finite and are analysed both numerically and asymptotically. For small values of proper radius of the compactified dimension, the leading terms of topological contributions are independent of the field mass and curvature coupling parameter, increasing by a power-law. In the opposite limit, the VEVs decay following a power-law in the general case. In the special case of a conformally coupled massless field the behavior is different. Unlike the VEV of field squared and vacuum energy density, the radial and azimuthal stresses are increasing by absolute value. As a consequence, the effects of nontrivial topology are strong for the stresses in this case at small values of radial coordinate.

1 Introduction

The investigation of field-theoretical effects in (2+1)-dimensional curved spacetimes is motivated by several reasons [1, 2, 3]. In backgrounds of this dimensionality the underlying laws of a system sometimes possess a certain symmetry, but the physically realized state of the system does not exhibit that symmetry. Particularly, there can occur phenomena where the laws of physics are not invariant under spatial inversion. Moreover, the strong correlations and topological effects in quantum many-body systems can cause fractionalization of the fundamental quantum numbers for the observable excitations. In addition, mechanisms can be provided for the generation of a topological mass for gauge bosons which is not accompanied with gauge symmetry breaking. There are compelling motivations in the context of cosmological research as well, such as the effective field theories describing the physics of compact subspace in Kaluza-Klein and braneworld models with extra dimensions. The Kaluza-Klein theory employs dimensional reduction by introducing an additional compactified spatial dimension, which allows for the unification of electromagnetism and gravity. The Kaluza-Klein dimensional reduction technic is employed for 2D elastic plates in [4]. The continuous development of planar condensed matter systems, such as carbon nanostructures, has increased significantly the interest towards 2D models. The long-wavelength degrees of freedom in those systems are described by 2D Dirac theory [5, 6].

In condensed matter physics, physical systems are typically modeled as residing in a flat spatial background. However, deformations such as stretching, compression, or torsion modify the distances

*E-mail: tigran.petrosyan@ysu.am

between points within a material. To describe these distortions, one can introduce an effective curved metric, which captures the system's local response to stress and strain. The associated curvature then serves as a mathematical analogue of a gravitational field, providing a geometric representation of mechanical deformations. Even in the absence of actual strain, it is often advantageous to introduce a fictitious gravitational field as a theoretical construct. This approach offers a systematic framework for evaluating the system's response to perturbations involving stress, momentum, or energy flow. As a concrete example, we can consider a real scalar field representing density fluctuations or an order parameter. By generalizing its flat-space Lagrangian to a curved-space form, one can define the energy-momentum tensor as the functional derivative of the action with respect to the background metric. Subsequently, differentiating the quantum generating functional with respect to this metric yields the correlation functions of the stress tensor, which are fundamental for analyzing energy-momentum transport and determining transport coefficients such as viscosity. For instance, the gravitational response of non-interacting 2D fermions in external magnetic field is evaluated in [7]. Thus, it becomes crucial to study the properties of quantum field states on various backgrounds.

In many two-dimensional quantum field theory models, including those relevant to condensed matter physics, the physical degrees of freedom are confined within finite regions by applying specific periodicity and boundary conditions. When topological defects are present, additional constraints on the fields are also introduced. Analyzing how boundary conditions influence quantum fields in (2+1) dimensions helps develop more realistic and practically useful models. Moreover, studying edge-related effects in (2+1)-dimensional spacetime offers valuable insights into the anti-de Sitter/conformal field theory (AdS/CFT) correspondence, where a (2+1)-dimensional quantum theory resides on the boundary of a (3+1)-dimensional AdS space. This perspective deepens our understanding of holography and its connection to string theory and quantum gravity. The boundary conditions alter the spectrum of quantum fluctuations, leading to boundary-dependent modifications in the expectation values of physical quantities. This shift is known as the Casimir effect, extensively studied for its fundamental importance and applications in nanoscale physics. Similar phenomena occur in systems with compact spatial dimensions, where the compactification of fields gives rise to topological Casimir effects, observed across a wide range of boundary and geometric configurations. The investigation of the non-trivial topology in (2+1)-dimensional models is currently a subject of active research. In particular, the 2D materials having negative constant curvature have various interesting condensed matter realizations. Recently, such materials have been used as simplified models for 2D black holes and wormholes [8, 9, 10, 11, 12]. New kinds of structures can be obtained by combining different geometries with rotational symmetry. For example, capped graphene nanotubes combine spherical and cylindrical geometries in their structure. The vacuum expectation values (VEVs) of the field squared and of the energy-momentum tensor for a quantum scalar field on that background are investigated in [13]. The generation of persistent currents on 2D curved tubes is a well-known effect [14, 15, 16, 17, 18, 19].

Rotationally symmetric (2+1)-dimensional spacetimes give a manageable setting to explore how mass, rotation, and curvature interact in general relativity [20, 21, 22]. The general (2+1)-dimensional rotationally symmetric spacetime can be described in coordinates (t, w, ϕ) by the line element $ds^2 = dt^2 - dw^2 - p^2(w)d\phi^2$, where $p(w)$ is some function of radial coordinate w . The simplest special case of this geometry corresponds to a cylinder with a constant radius (in this case $p(w)$ is equal to the cylinder radius). If the function $p(w)$ is linear, $p(w) = \alpha w$, then one has either a plane ($\alpha = 1$) or a cone with an opening angle $2\pi\alpha$ ($\alpha < 1$). The fermionic condensate and currents for a 2D fermionic field localized on a conical spacetime with two parallel circular boundaries are discussed in [23, 24] (see also [25] for finite temperature fermionic currents in case of one boundary). The constant positive curvature space is another example of the general geometry corresponding to a sphere of radius a . In the latter case one has $p(w) = L \sin(w/a)$, with L being a constant having the dimension of length. The corresponding condensed matter realizations include fullerenes and topological insulators with spherical surfaces. The VEVs of the field squared and of the energy-momentum tensor for a complex scalar field on the background of de Sitter spacetime and Milne universe in the presence

of a spherical surface are studied in [26, 27, 28]. As another special case the constant negative curvature spaces can be mentioned. In this case three different subcases can be realized: the elliptic pseudosphere ($p(w) = L \sinh(w/a)$), the hyperbolic pseudosphere ($p(w) = L \cosh(w/a)$) and the Beltrami pseudosphere ($p(w) = L e^{w/a}$). The solution of Einstein-Maxwell equations with negative cosmological constant in (2+1)-dimensions corresponds to the lower-dimensional analog of a black hole, known as BTZ black hole. The latter is described by a rotationally symmetric spacetime with constant negative curvature. The corresponding black hole entropy and temperature for the cases of vanishing and nonzero charges are evaluated in [29] (see also [30, 31, 32, 33]). It is shown that for negative values of the mass there is a naked conical singularity. However, it disappears in the special case of vanishing angular momentum, provided that the mass is precisely -1 . In this bound state the line element coincides with that of the (2+1)-dimensional AdS spacetime. The investigation of BTZ black hole provides insight especially in quantum properties of black holes. The renormalized energy-momentum tensor for strongly coupled quantum conformal fields in the rotating BTZ black hole is presented in [34]. In the present paper we consider the (2+1)-dimensional Beltrami pseudosphere as a background geometry, and we are interested in the effects induced by the spatial topology and curvature on the vacuum characteristics of a massive complex scalar field.

The paper is organized as follows. In the next section we describe the background geometry and present the expressions for the Hadamard function. By using the Hadamard function, the VEV of the field squared is evaluated in Section 3. The corresponding expressions for the diagonal components of the VEV of energy-momentum tensor, as well as the asymptotic and numerical analysis of the corresponding topological contributions is presented in Section 4. The main results of the paper are summarized in Section 5.

2 Problem geometry and Hadamard function

The (2+1)-dimensional Beltrami pseudosphere is described by the spacetime coordinates (t, r, ϕ) with the line element [20]

$$ds^2 = dt^2 - \frac{a^2}{r^2} (dr^2 + L^2 d\phi^2), \quad (2.1)$$

where a is the curvature radius and L is a constant with dimension of length. The radial coordinate is related to the coordinate w mentioned in the Section 1 as $r = a e^{-w/a}$, $0 \leq r < \infty$. For the part of the manifold that can be embedded in a 3-dimensional Euclidean space one has $r \geq L$. For a given r the dimensionless ratio aL/r corresponds to the proper radius of the compactified dimension. The nonzero components of the Ricci tensor and the Ricci scalar have the form

$$R_1^1 = R_2^2 = -\frac{1}{a^2}, \quad R = -\frac{2}{a^2}. \quad (2.2)$$

The Beltrami pseudosphere depicted in Fig. 1 represents a constant negative curvature space with the Gaussian curvature $K = R/2$.

We consider a massive scalar field $\varphi(x) \equiv \varphi(t, r, \phi)$ on the background of the Beltrami pseudosphere. The field obeys the equation

$$(\nabla^p \nabla_p + m^2 + \xi R) \varphi(x) = 0, \quad (2.3)$$

where m is the field mass, ξ is the curvature coupling parameter and ∇_p is the covariant derivative operator. The field obeys also the quasiperiodicity condition

$$\varphi(t, r, \phi + 2\pi) = e^{i\alpha_p} \varphi(t, r, \phi), \quad (2.4)$$

with a constant phase α_p . The latter can be interpreted physically as the existence of a magnetic flux in the embedding space, threading the Beltrami pseudosphere. The corresponding two-point

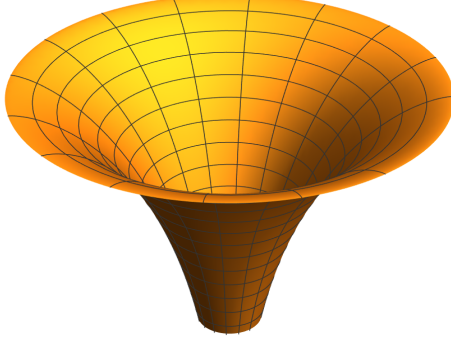


Figure 1: The Beltrami pseudosphere embedded in a 3-dimensional Euclidean space.

Hadamard function has the form [20]

$$G(x, x') = \frac{a^{-2}}{2\pi} \sum_{l=-\infty}^{\infty} e^{-il\alpha_p} \int_0^{\infty} d\nu \frac{\nu}{\omega} \tanh(\pi\nu) \cos(\omega\Delta t) P_{i\nu-1/2} \left(\frac{r^2 + r'^2 + L^2 (\Delta\phi + 2\pi l)^2}{2rr'} \right), \quad (2.5)$$

where $P_{\mu}(z)$ is the Legendre function of the first kind, $\Delta\phi = \phi - \phi'$, $\Delta t = t - t'$, $\omega = \sqrt{\nu^2 + \nu_m^2}/a$ and $\nu_m^2 = m^2 a^2 + 1/4 - 2\xi$. The term with $l = 0$ in (2.5) corresponds to the Hadamard function in the geometry with an uncompactified coordinate ϕ . The latter part is given as

$$G_0(x, x') = \frac{1}{2\pi a} \int_0^{\infty} d\nu \frac{\nu}{\sqrt{\nu^2 + \nu_m^2}} \tanh(\nu\pi) \cos(\omega\Delta t) P_{i\nu-1/2} \left(\frac{r^2 + r'^2 + (L\Delta\phi)^2}{2rr'} \right). \quad (2.6)$$

As an alternative representation for the Hadamard function we use the expression

$$G(x, x') = \frac{1}{\pi^2 a} \sum_{l=-\infty}^{\infty} e^{il\alpha_p} \int_{\nu_m}^{\infty} d\nu \frac{\nu \cosh\left(\sqrt{\nu^2 - \nu_m^2} \Delta t/a\right)}{\sqrt{\nu^2 - \nu_m^2}} Q_{\nu-1/2} \left(\frac{r^2 + r'^2 + L^2 (\Delta\phi - 2\pi l)^2}{2rr'} \right), \quad (2.7)$$

where again the Hadamard function in the geometry with uncompactified coordinate ϕ , $G_0(x, x')$, is given by the term with $l = 0$. Here $Q_{\mu}(z)$ is the associated Legendre function of the second kind. The Hadamard function for a general rotationally symmetric geometry can be obtained by the mode summation method by applying the generalized Abel-Plana formula [20, 35].

3 VEV of field squared

Having the expression for the Hadamard function we can evaluate the characteristics of the scalar vacuum. In this section we will investigate the VEV of the field squared which can be found by the formula

$$\langle \varphi^2 \rangle = \frac{1}{2} \lim_{x' \rightarrow x} G(x, x'). \quad (3.1)$$

Substituting here (2.5) we get

$$\langle \varphi^2 \rangle = \frac{1}{4\pi a} \int_0^{\infty} d\nu \frac{\nu \tanh(\pi\nu)}{\sqrt{\nu^2 + \nu_m^2}} + \frac{1}{2\pi a} \sum_{l=1}^{\infty} \cos(l\alpha_p) \int_0^{\infty} d\nu \frac{\nu}{\sqrt{\nu^2 + \nu_m^2}} \tanh(\pi\nu) P_{i\nu-1/2}(x), \quad (3.2)$$

where x is defined as

$$x \equiv x_l(r) = 1 + 2 \left(\frac{\pi l L}{r} \right)^2, \quad l \neq 0. \quad (3.3)$$

The first term in (3.2), which is divergent, corresponds to the geometry with an uncompactified azimuthal coordinate and it does not depend on the compactification length and radial coordinate. The dependence on L and r is contained in the last term of (3.2) and it appears in the form of the ratio L/r . The latter presents the proper length of the compact dimension measured in units of a . Hence the covariant d'Alembertian of the VEV has the form

$$\nabla_p \nabla^p \langle \varphi^2 \rangle = \frac{1}{2\pi a^3} \sum_{l=1}^{\infty} \cos(l\alpha_p) \int_0^{\infty} d\nu \frac{\nu}{\sqrt{\nu^2 + \nu_m^2}} \tanh(\pi\nu) \hat{F}_{\square} P_{i\nu-1/2}(x), \quad (3.4)$$

with the operator \hat{F}_{\square} defined as

$$\hat{F}_{\square} = -2(x-1) [2(x-1)\partial_x^2 + 3\partial_x]. \quad (3.5)$$

An alternative representation suitable for numerical evaluations can be obtained by using (2.7). The latter gives

$$\langle \varphi^2 \rangle = \frac{1}{2\pi^2 a} \int_{\nu_m}^{\infty} d\nu \frac{\nu}{\sqrt{\nu^2 - \nu_m^2}} \lim_{x \rightarrow 1} Q_{\nu-1/2}(x) + \langle \varphi^2 \rangle_c, \quad (3.6)$$

where the first term is again divergent and needs a renormalization. The second term on the right hand side of (3.6) corresponds to the compact counterpart in the VEV of field squared and has the form

$$\langle \varphi^2 \rangle_c = \frac{1}{\pi^2 a} \sum_{l=1}^{\infty} \cos(l\alpha_p) \int_{\nu_m}^{\infty} d\nu \frac{\nu}{\sqrt{\nu^2 - \nu_m^2}} Q_{\nu-1/2}(x). \quad (3.7)$$

In this form for the corresponding covariant d'Alembertian we obtain

$$\nabla_p \nabla^p \langle \varphi^2 \rangle = \frac{1}{\pi^2 a^3} \sum_{l=1}^{\infty} \cos(l\alpha_p) \int_{\nu_m}^{\infty} d\nu \frac{\nu}{\sqrt{\nu^2 - \nu_m^2}} \hat{F}_{\square} Q_{\nu-1/2}(x), \quad (3.8)$$

with the same operator \hat{F}_{\square} defined as (3.5). In this paper our main interest are the topological contributions to the VEVs of field squared and energy-momentum tensor.

As another characteristic of the vacuum state we can consider the VEV of the current density $\langle 0|j_k(x)|0 \rangle \equiv \langle j_k(x) \rangle$, where

$$j_k(x) = ie[\varphi^\dagger(x)\partial_k\varphi(x) - (\partial_k\varphi(x))^\dagger\varphi(x)] \quad (3.9)$$

is the corresponding operator and e is the charge of the field quantum. This VEV can be obtained from the Hadamard function by the formula

$$\langle j_k(x) \rangle = \frac{i}{2} e \lim_{x' \rightarrow x} (\partial_k - \partial'_k) G(x, x'). \quad (3.10)$$

According to [20] the only nonzero component is the VEV of the current density in the compact dimension $\langle j_2 \rangle$. The corresponding physical component $\langle j^\phi \rangle = -r\langle j_2 \rangle/La$ is given as

$$\langle j^\phi \rangle = -\frac{4eL}{\pi r a^2} \sum_{l=1}^{\infty} l \sin(l\alpha_p) \int_{\nu_m}^{\infty} d\nu \nu \frac{Q'_{\nu-1/2} \left(1 + 2 \left(\frac{\pi l L}{r} \right)^2 \right)}{\sqrt{\nu^2 - \nu_m^2}}, \quad (3.11)$$

where the prime means the derivative with respect to the argument of the function. As seen from (3.7) and (3.11), the VEV of the field squared is an even function of α_p , whereas the VEV of the current density is an odd function.

Let us consider the behavior of $\langle \varphi^2 \rangle_c$ in the asymptotic regions of the ratio r/L . For $r/L \ll 1$ the argument of the Legendre function in (3.7) is large and we use the formula [36]

$$Q_{\nu-1/2}(x) \approx \frac{\sqrt{\pi}\Gamma(\nu+1/2)}{\Gamma(\nu+1)(2x)^{\nu+1/2}}, \quad x \gg 1. \quad (3.12)$$

In the leading order this gives

$$\langle \varphi^2 \rangle_c \approx \frac{\Gamma(\nu_m+1/2)}{2\pi a \Gamma(\nu_m) \sqrt{\nu_m \ln(2\pi L/r)}} \left(\frac{r}{2\pi L}\right)^{2\nu_m+1} \sum_{l=1}^{\infty} \frac{\cos(l\alpha_p)}{l^{2\nu_m+1}}, \quad (3.13)$$

and $\langle \varphi^2 \rangle_c$ tends to zero like $(r/L)^{2\nu_m+1}$. The corresponding leading term in case of conformally coupled massless field ($\nu_m = 0$) is given as

$$\langle \varphi^2 \rangle_c \approx \frac{1}{4\pi^2 a} \frac{1}{\ln(2\pi L/r)} \frac{r}{L} \sum_{l=1}^{\infty} \frac{1}{l} \cos(l\alpha_p). \quad (3.14)$$

Note that in the limit under consideration $L/r \gg 1$ and this corresponds to large values of the proper length of compact dimension compared to the curvature radius a .

In the opposite limit $r/L \gg 1$ the dominant contribution to the integral in (3.7) comes from large ν and we use the uniform asymptotic approximation [36]

$$Q_{\nu-1/2}(\cosh u) \approx \left(\frac{u}{\sinh u}\right)^{1/2} K_0(\nu u), \quad \nu \gg 1. \quad (3.15)$$

After that we perform integration by ν and for the leading order term we obtain

$$\langle \varphi^2 \rangle_c \approx \frac{r/L}{4\pi^2 a} \sum_{l=1}^{\infty} \frac{1}{l} \cos(l\alpha_p). \quad (3.16)$$

This result coincides with the corresponding VEV for the cylindrical tube with a constant radius aL/r . The dominant contribution comes from the modes with high momenta along the compact dimension and the influence of the curvature on those modes is weak.

It would be useful to compare numerically the compact counterpart of the VEV of field squared (3.7) with the corresponding azimuthal current density (3.11). The VEVs $\langle \varphi^2 \rangle_c$ and $\langle j^\phi \rangle$ versus the radial coordinate in the form of the ratio L/r are shown in the left and right panels of Fig. 2. The graphs are plotted for conformally and minimally coupled massless fields assuming that the phase in the quasiperiodicity condition is equal to $\pi/2$. The numbers near curves represent the values of the curvature coupling parameter ξ . Both VEVs diverge and have opposite signs for large values of r/L (the VEV of field squared diverges as r/L , whereas $\langle j^\phi \rangle$ is increasing faster, as $(r/L)^2$). In Fig. 3 the same quantities are presented versus field mass in the units of a^{-1} for the values of parameters $\alpha_p = 2\pi/5$ and $L/r = 0.5$. Both VEVs are vanishing for large masses, however $\langle \varphi^2 \rangle_c$ has a maximum value for nonzero field mass. The same VEVs are depicted in Fig. 4, as functions of the parameter $\alpha_p/2\pi$ for conformally and minimally coupled fields assuming that $L/r = 0.5$ and $ma = 0.5$. As mentioned above, the VEV of field squared is an even function of the phase, whereas the VEV of the current density is an odd function.

4 VEV of energy-momentum tensor

As another important characteristic of the vacuum state we consider the VEV of energy-momentum tensor. The latter can be obtained with the help of the formula [1]

$$\langle T_{ik} \rangle = \frac{1}{4} \lim_{x' \rightarrow x} (\partial_{i'} \partial_k + \partial_{k'} \partial_i) G(x, x') + \left(\xi - \frac{1}{4}\right) g_{ik} \nabla_p \nabla^p \langle \varphi^2 \rangle - \xi \nabla_i \nabla_k \langle \varphi^2 \rangle - \xi R_{ik} \langle \varphi^2 \rangle, \quad (4.1)$$

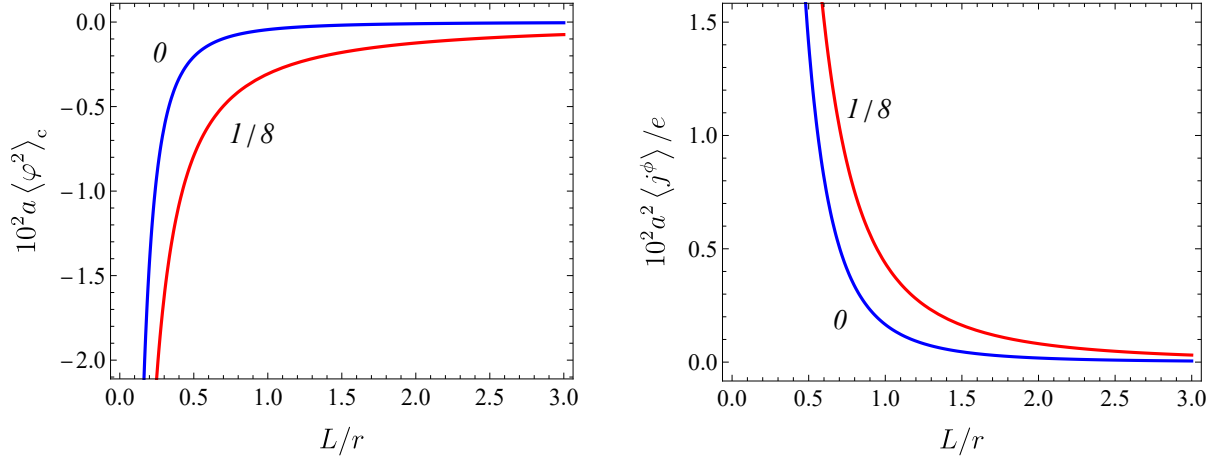


Figure 2: The VEV of field squared (left panel) and the azimuthal current density (right panel) as a function of the L/r for conformally ($\xi = 1/8$) and minimally ($\xi = 0$) coupled massless fields and for fixed $\alpha_p = \pi/2$.

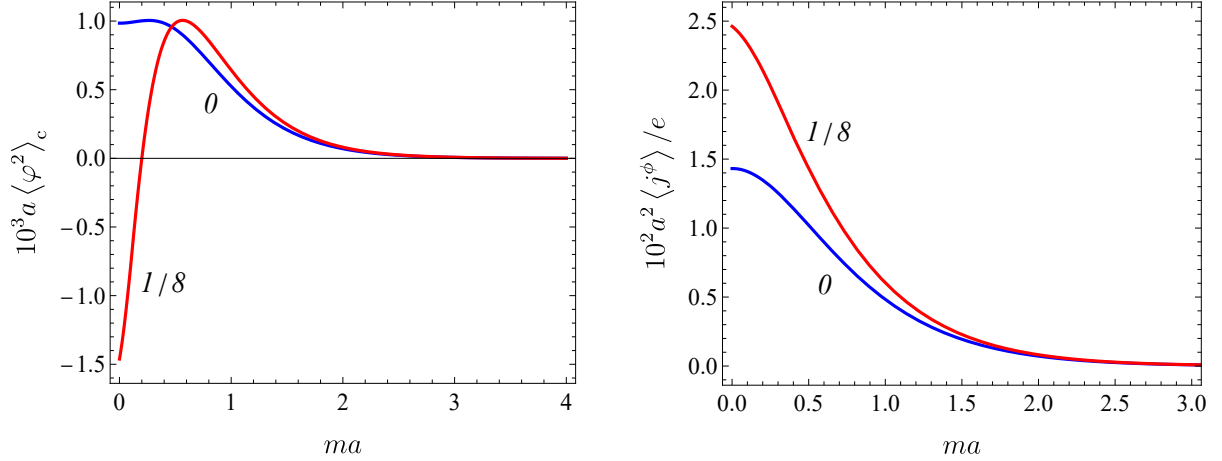


Figure 3: The VEV of field squared (left panel) and the azimuthal current density (right panel) as a function of the mass for conformally ($\xi = 1/8$) and minimally ($\xi = 0$) coupled fields with $L/r = 0.5$ and $\alpha_p = 2\pi/5$.

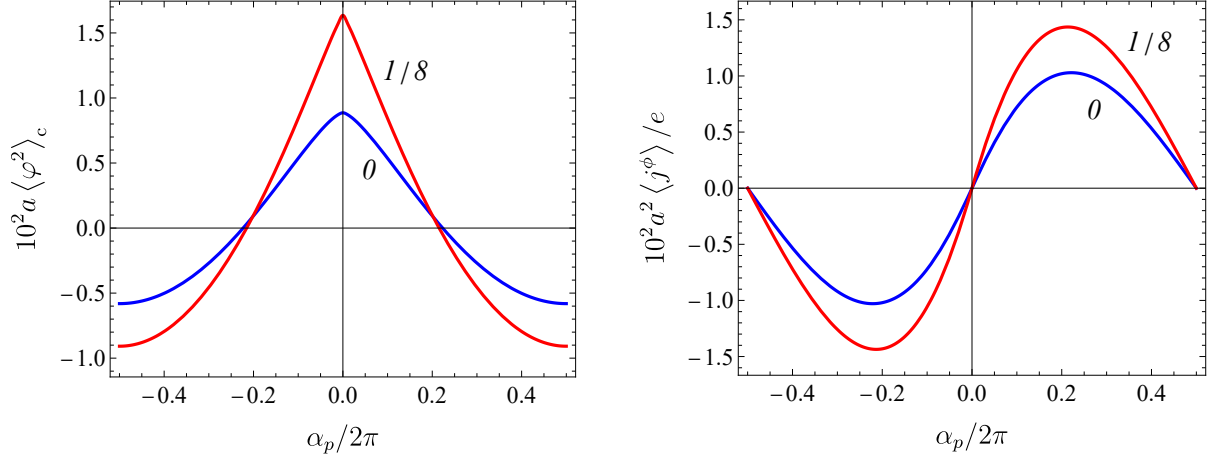


Figure 4: The VEV of field squared (left panel) and the azimuthal current density (right panel) as a function of the phase in the quasiperiodicity condition for conformally ($\xi = 1/8$) and minimally ($\xi = 0$) coupled fields with $L/r = 0.5$ and $ma = 0.5$.

where g_{ik} is the metric tensor and ∇_i is the covariant derivative. The straightforward calculation with the use of the expressions (2.5) and (3.2) gives the following expressions for the nonzero components (no summation over i):

$$\begin{aligned} \langle T_i^i \rangle &= \frac{1}{2\pi a^3} \int_0^\infty d\nu \frac{\nu}{\sqrt{\nu^2 + \nu_m^2}} \tanh(\pi\nu) F_i^{(0)}(\nu) \\ &+ \frac{1}{2\pi a^3} \sum_{l=1}^\infty \cos(l\alpha_p) \int_0^\infty d\nu \frac{\nu}{\sqrt{\nu^2 + \nu_m^2}} \tanh(\pi\nu) \hat{F}_i P_{i\nu-1/2}(x), \end{aligned} \quad (4.2)$$

where

$$F_0^{(0)}(\nu) = \frac{1}{2}(\nu^2 + \nu_m^2), \quad F_1^{(0)}(\nu) = F_2^{(0)}(\nu) = \frac{1}{4} \left(-\nu^2 + 2\xi - \frac{1}{4} \right), \quad (4.3)$$

and the operators \hat{F}_i , $i = 0, 1, 2$, are defined as

$$\hat{F}_0 = -2 \left(\xi - \frac{1}{4} \right) (x-1) [2(x-1)\partial_x^2 + 3\partial_x] + \nu^2 + \nu_m^2, \quad (4.4)$$

$$\hat{F}_1 = -\frac{1}{2} [(4\xi - 1)x - 4\xi - 1] \partial_x + \xi, \quad (4.5)$$

$$\hat{F}_2 = -\frac{1}{2} \{ 2(x-1)[(4\xi - 1)x - 4\xi - 1] \partial_x^2 + [(8\xi - 3)x - 8\xi + 1] \partial_x - 2\xi \}. \quad (4.6)$$

Similar to the case of the field squared, the vacuum energy-momentum tensor is an even function of α_p . The VEV of energy-momentum tensor (4.2) obeys the trace relation

$$\langle T_k^k \rangle = \left[2(\xi - 1/8) \nabla_k \nabla^k + m^2 \right] \langle \varphi^2 \rangle. \quad (4.7)$$

The covariant conservation equation $\nabla_k \langle T_i^k \rangle = 0$ with $i = 1$ gives the relation

$$\langle T_2^2 \rangle = \left(1 - r \frac{\partial}{\partial r} \right) \langle T_1^1 \rangle, \quad (4.8)$$

which is satisfied by the expression (4.2). The remaining components of the conservation equation are reduced to a trivial identity.

An alternative form for the VEVs can be obtained by means of the expressions (2.7) and (3.6):

$$\langle T_i^i \rangle = \frac{1}{\pi^2 a^3} \int_{\nu_m}^{\infty} d\nu \frac{\nu}{\sqrt{\nu^2 - \nu_m^2}} R_i^{(0)}(\nu) \lim_{x \rightarrow 1} Q_{\nu-1/2}(x) + \langle T_i^i \rangle_c, \quad (4.9)$$

with

$$R_0^{(0)}(\nu) = F_0^{(0)}(\nu) - \nu^2, \quad R_1^{(0)}(\nu) = R_2^{(0)}(\nu) = F_1^{(0)}(\nu) + \frac{\nu^2}{2},$$

and with the compactified part $\langle T_i^i \rangle_c$ having the form

$$\langle T_i^i \rangle_c = \frac{1}{\pi^2 a^3} \sum_{l=1}^{\infty} \cos(l\alpha_p) \int_{\nu_m}^{\infty} d\nu \frac{\nu}{\sqrt{\nu^2 - \nu_m^2}} \hat{R}_i Q_{\nu-1/2}(x). \quad (4.10)$$

Here the operators \hat{R}_i , $i = 0, 1, 2$, are defined as

$$\hat{R}_i = \hat{F}_i - 2\nu^2 \delta_{0i}, \quad (4.11)$$

with \hat{F}_i given by (4.4)-(4.6) and δ_{0i} being the Kronecker delta.

As an important special case we consider the conformally coupled massless field. In this case one has $\nu_m = 0$, $\xi = 1/8$ and the VEVs are given as

$$\begin{aligned} \langle T_i^i \rangle &= \frac{1}{2\pi a^3} \int_0^{\infty} d\nu \tanh(\pi\nu) F_{i,c}^{(0)}(\nu) + \frac{1}{2\pi a^3} \sum_{l=1}^{\infty} \cos(l\alpha_p) \int_0^{\infty} d\nu \tanh(\pi\nu) \hat{F}_{i,c} P_{i\nu-1/2}(x) \\ &= \frac{1}{\pi^2 a^3} \int_0^{\infty} d\nu R_{i,c}^{(0)}(\nu) \lim_{x \rightarrow 1} Q_{\nu-1/2}(x) + \frac{1}{\pi^2 a^3} \sum_{l=1}^{\infty} \cos(l\alpha_p) \int_0^{\infty} d\nu \hat{R}_{i,c} Q_{\nu-1/2}(x), \end{aligned} \quad (4.12)$$

with

$$F_{0,c}^{(0)}(\nu) = -2F_{1,c}^{(0)}(\nu) = -2F_{2,c}^{(0)}(\nu) = -R_{0,c}^{(0)}(\nu) = 2R_{1,c}^{(0)}(\nu) = 2R_{2,c}^{(0)}(\nu) = \frac{\nu^2}{2}, \quad (4.13)$$

and

$$\begin{aligned} \hat{F}_{0,c} &= \hat{R}_{0,c} + 2\nu^2 = \frac{1}{4}(x-1)[2(x-1)\partial_x^2 + 3\partial_x] + \nu^2, \\ \hat{F}_{1,c} &= \hat{R}_{1,c} = \frac{1}{8}[2(x+3)\partial_x + 1], \\ \hat{F}_{2,c} &= \hat{R}_{2,c} = \frac{1}{8}[4(x-1)(x+3)\partial_x^2 + 8x\partial_x + 1]. \end{aligned}$$

Note that the geometry given by (2.1) is conformally related to the 2D Rindler spacetime described by the line element $ds_{\text{R}}^2 = r^2 d\tau^2 - dr^2 - dy^2$ with dimensionless time coordinate $\tau = t/a$ and compact coordinate $y = L\phi$ (for the VEVs in $(D+1)$ -dimensional Rindler spacetime with general number of compact dimensions see [37]), i.e. $ds^2 = (a/r)^2 ds_{\text{R}}^2$. Thus, the diagonal components of the topological contributions in the VEV of energy-momentum tensor in the locally Rindler spacetime, $\langle T_k^k \rangle_{\text{R},c}$, are related to the components $\langle T_k^k \rangle_c$ by the formulae (no summation over k)

$$\langle T_k^k \rangle_{\text{R},c} = (a/r)^3 \langle T_k^k \rangle_c, \quad k = 0, 1, 2. \quad (4.14)$$

Now, we discuss the asymptotic behavior of the compact counterparts in the VEV of energy-momentum tensor for the limiting cases of the ratio r/L . For $r/L \ll 1$ one has the approximations

$$\langle T_0^0 \rangle_c \approx (1 - 4\xi) \nu_m (\nu_m + 1/2) T(2\pi L/r), \quad (4.15)$$

$$\langle T_1^1 \rangle_c \approx [(2\xi - 1/2) (\nu_m + 1/2) + \xi] T(2\pi L/r), \quad (4.16)$$

$$\langle T_2^2 \rangle_c \approx \{\xi - [4\xi (\nu_m + 1/2) - \nu_m] (\nu_m + 1/2)\} T(2\pi L/r), \quad (4.17)$$

with the function $T(z)$ defined as

$$T(z) = \frac{\sqrt{\nu_m} \Gamma(\nu_m + 1/2)}{2\pi a^3 \Gamma(\nu_m + 1)} \frac{z^{-2\nu_m - 1}}{\sqrt{\ln z}} \sum_{l=1}^{\infty} \frac{\cos(l\alpha_p)}{l^{2\nu_m + 1}}. \quad (4.18)$$

In the case of a conformally coupled massless field the corresponding leading terms have the form

$$\langle T_0^0 \rangle_c \approx -\langle T_1^1 \rangle_c \approx \ln(2\pi L/r) \langle T_2^2 \rangle_c \approx \frac{r/L}{32\pi^2 a^3 [\ln(2\pi L/r)]^2} \sum_{l=1}^{\infty} \frac{1}{l} \cos(l\alpha_p). \quad (4.19)$$

The approximations for the opposite limit $r/L \gg 1$ are obtained similar to (3.16) and are given as

$$\langle T_0^0 \rangle_c \approx \langle T_1^1 \rangle_c \approx -\frac{1}{2} \langle T_2^2 \rangle_c \approx -\frac{(r/L)^3}{16\pi^4 a^3} \sum_{l=1}^{\infty} \frac{\cos(l\alpha_p)}{l^3}, \quad (4.20)$$

which coincide with the VEVs for a cylindrical tube with constant radius aL/r .

Here we discuss some numerical examples presented for the compact counterpart in the first diagonal component of the VEV of the energy-momentum tensor corresponding to the energy density. The left panel of Fig. 5 presents the dependence of the energy density on the mass of the field for the parameters $L/r = 0.5$ and $\alpha_p = 2\pi/5$. The right panel displays the energy density versus $\alpha_p/2\pi$ for the same value of L/r and for $ma = 0.5$. On both panels the numbers near the curves are the corresponding values of the curvature coupling parameter. The corresponding dependences for vacuum stresses $\langle T_i^i \rangle_c$, $i = 1, 2$ (no summation over i) are depicted in Fig. 6. Here, the full and dashed curves correspond to $\langle T_1^1 \rangle_c$ and $\langle T_2^2 \rangle_c$, respectively. In Fig. 7, the left panel shows the dependence of the

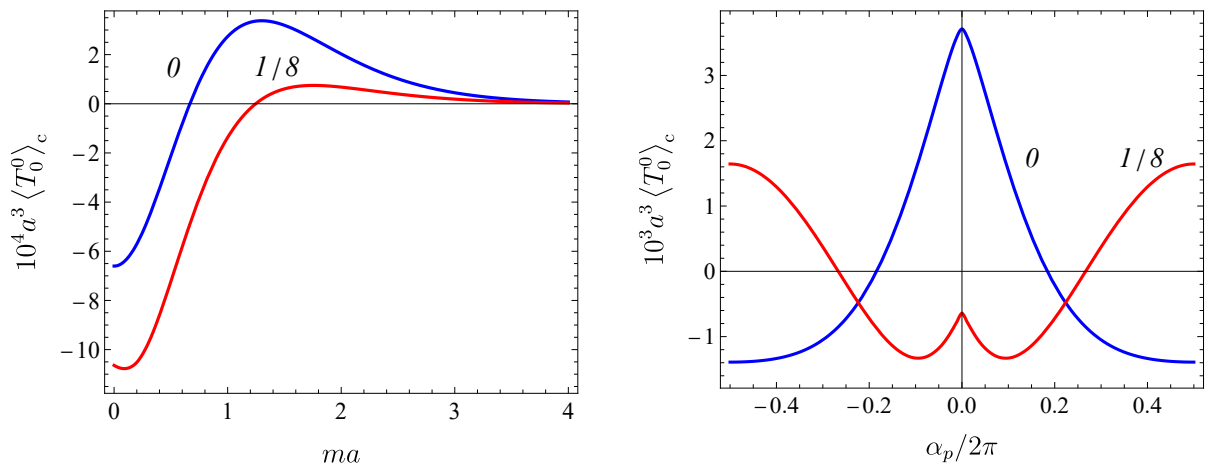


Figure 5: The energy density as a function of the mass (left panel) and of the phase in the quasiperiodicity condition (right panel) for $L/r = 0.5$. For the left panel we have taken $\alpha_p = 2\pi/5$ and for the right panel $ma = 0.5$.

energy density on the ratio L/r for minimally and conformally coupled massless fields. The graphs are plotted for $\alpha_p = \pi/2$. As was expected, the energy density tends to zero in the limit $L/r \rightarrow \infty$. The corresponding dependences for vacuum stresses are presented on the right panel. Again, the full (dashed) curves represent the radial (azimuthal) stress.

5 Conclusion

We have investigated the combined effects of spatial curvature and topology on the properties of the vacuum state for a charged scalar field localized on the (2+1)-dimensional Beltrami pseudosphere.

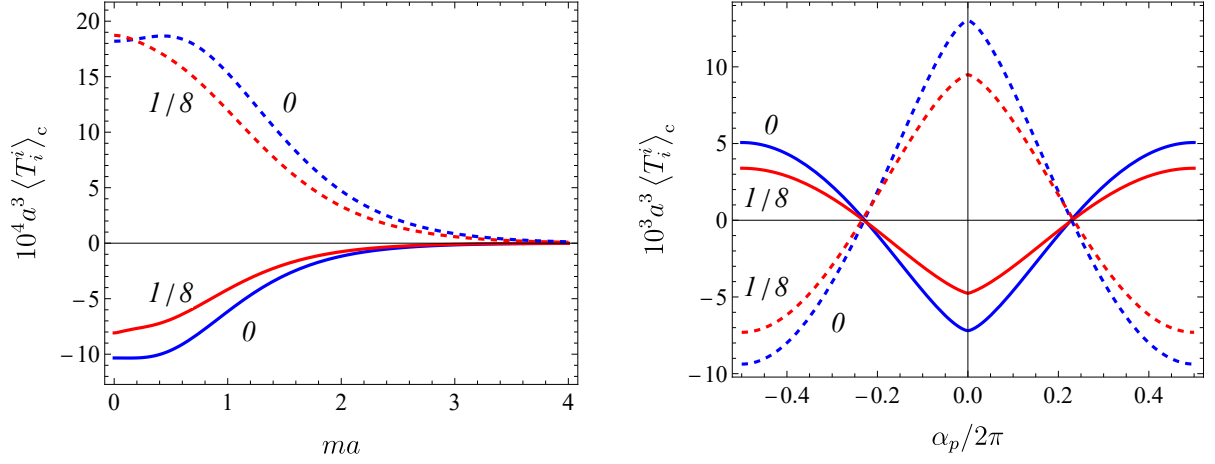


Figure 6: Same as in Fig. 5 for $\langle T_1^1 \rangle_c$ (full curves) and $\langle T_2^2 \rangle_c$ (dashed curves).

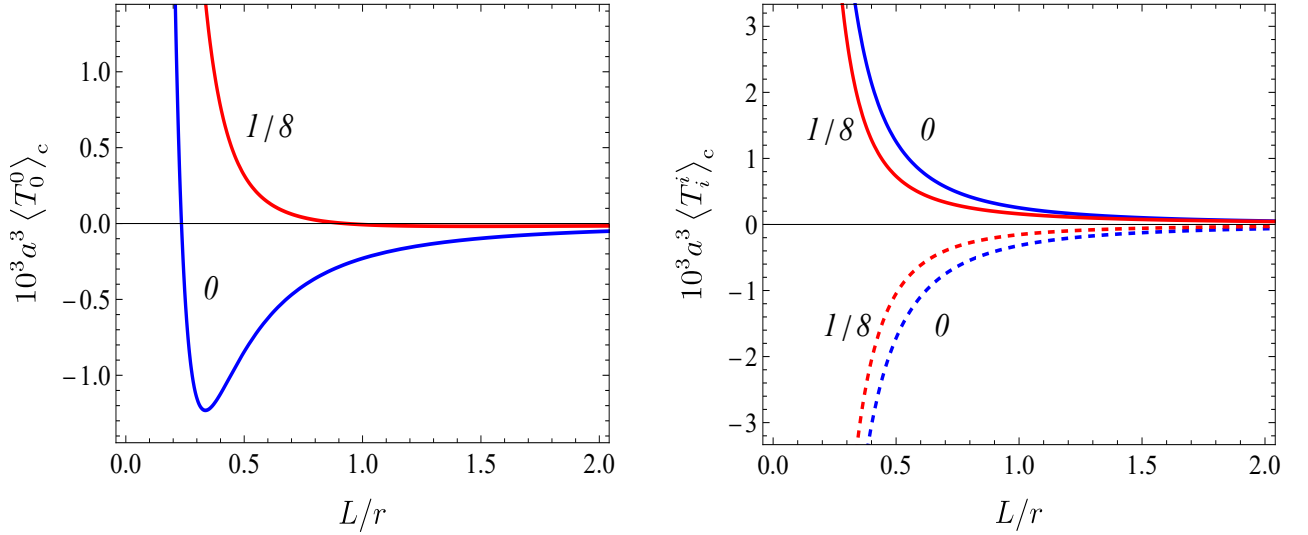


Figure 7: The vacuum energy density (left panel) and vacuum stresses (right panel) versus L/r for conformally ($\xi = 1/8$) and minimally ($\xi = 0$) coupled massless fields and for fixed $\alpha_p = \pi/2$. Full and dashed curves on the right panel correspond to $\langle T_1^1 \rangle_c$ and $\langle T_2^2 \rangle_c$, respectively.

The corresponding geometry is described by the line element (2.1). It is assumed that the field obeys the quasiperiodicity condition (2.4) where the phase is constant. With the help of the expressions obtained in [20] for the two-point Hadamard function, two equivalent representations are obtained for the important physical characteristics of the vacuum state. As such characteristics we have considered the VEVs of the field squared and of the energy-momentum tensor. The corresponding expressions are given by (3.2) and (4.2) for the first representation, and (3.6) and (4.9) for the second one. The VEVs are decomposed into compactified and uncompactified parts. The latter parts are divergent, whereas the compact counterparts are finite. Thus, the renormalization of the VEVs is reduced to that for the uncompactified parts only. As an important special case we have discussed the conformally coupled massless scalar field. The geometry for the Beltrami pseudosphere is conformally related to the (2+1)-dimensional Rindler spacetime and the corresponding VEVs of the energy-momentum tensor in these two spacetimes are related by the formula (4.14) for a conformally coupled massless field.

In addition, the topological contributions have been analysed asymptotically for the limiting values of the ratio r/L . For a given r the dimensionless ratio r/L corresponds to the inverse of the proper radius of the compactified dimension measured in units of the curvature radius. In the case of $r/L \ll 1$ the VEVs are approximated as (3.13) and (4.15)-(4.17). In this limit, the decay of the compact counterpart in the energy density as a function of r/L follows a power-law, as $(r/L)^{2\nu_m+1}$. The formulae (4.15)-(4.17) are not applicable for the conformally coupled massless case and the expressions (4.19) are provided for that case. Contrary to the VEV of the field squared and the energy density, the absolute values of the radial and azimuthal stresses are increasing as the ratio r/L tends to zero, therefore the effect of nontrivial topology is strong for the stresses at small values of the radial coordinate in the conformally coupled massless case. The nontrivial topology is essential also in the opposite asymptotic limit, $r/L \gg 1$. The corresponding leading terms are given as (3.16) and (4.20). The approximate expressions are independent of the mass m and of the curvature coupling parameter ξ . The magnitudes of the VEVs are increasing by a power-law as the ratio r/L takes large values.

Acknowledgments

The research was supported by the Higher Education and Science Committee of MESCS RA (Research projects No. 21AG-1C047 and No. 24FP-3B021).

References

- [1] N.D. Birrell, P.C.W. Davies, *Quantum Fields in Curved Space* (Cambridge University Press, Cambridge, England, 1982).
- [2] A.A. Grib, S.G. Mamayev, V.M. Mostepanenko, *Vacuum Quantum Effects in Strong Fields* (Friedmann Laboratory Publishing, St. Petersburg, 1994).
- [3] L.E. Parker, D.J. Toms, *Quantum Field Theory in Curved Spacetime* (Cambridge University Press, Cambridge, England, 2009).
- [4] M. Adda-Bedia, E. Katzav, Kaluza–Klein dimensional reduction from elasticity theory of crumpled paper, *Eur. Phys. J. Plus* **138**, 198 (2023).
- [5] V.P. Gusynin, S.G. Sharapov, J.P. Carbotte, AC conductivity of graphene: From tight-binding model to 2+1-dimensional quantum electrodynamics, *Int. J. Mod. Phys. B* **21**, 4611 (2007).
- [6] A.H. Castro Neto, F. Guinea, N.M.R. Peres, K.S. Novoselov, A.K. Geim, The electronic properties of graphene, *Rev. Mod. Phys.* **81**, 109 (2009).

- [7] A.G. Abanov, A. Gromov, Electromagnetic and gravitational responses of two-dimensional non-interacting electrons in background magnetic field, *Phys. Rev. B* **90**, 014435 (2014).
- [8] A. Iorio, G. Lambiase, The Hawking-Unruh phenomenon on graphene, *Phys. Lett. B* **716**, 334 (2012).
- [9] A. Iorio, G. Lambiase, Quantum field theory in curved graphene spacetimes, Lobachevsky geometry, Weyl symmetry, Hawking effect, and all that, *Phys. Rev. D* **90**, 025006 (2014).
- [10] A. Gallerati, Negative-curvature spacetime solutions for graphene, *J. Phys.: Condens. Matter* **33**, 135501 (2021).
- [11] A. Gallerati, Graphene, Dirac equation and analogue gravity, *Phys. Scr.* **97**, 064005 (2022).
- [12] G. Alencar, V.B. Bezerra, C.R. Muniz, Casimir wormholes in 2+1 dimensions with applications to the graphene, *Eur. Phys. J. C* **81**, 924 (2021).
- [13] E.R. Bezerra de Mello, A.A. Saharian, Casimir effect in hemisphere capped tubes, *Int. J. Theor. Phys.* **55**, 1167 (2016).
- [14] G.V. Dunne, *Topological Aspects of Low Dimensional Systems* (Springer, Berlin, 1999).
- [15] Y. Imry, *Introduction to Mesoscopic Physics* (Oxford University Press, New York, USA, 2008).
- [16] V.M. Fomin (Ed.), *Physics of Quantum Rings* (Springer International Publishing, Cham, Switzerland, 2018).
- [17] A.A. Saharian, Vacuum currents for a scalar field in models with compact dimensions, *Symmetry* **16**, 92 (2024).
- [18] A.C. Bleszynski-Jayich, W.E. Shanks, B. Peaudecerf, E. Ginossar, F. von Oppen, L. Glazman, J.G.E. Harris, Persistent currents in normal metal rings, *Science* **326**, 272 (2009).
- [19] H. Bluhm, N.C. Koshnick, J.A. Bert, M.E. Huber, K.A. Moler, Persistent currents in normal metal rings, *Phys. Rev. Lett.* **102**, 136802 (2009).
- [20] A.A. Saharian, Vacuum currents in curved tubes, *Phys. Rev. D* **110**, 065020 (2024).
- [21] A.A. Saharian, G.V. Mirzoyan, Vacuum currents in elliptic pseudosphere tubes, *Nucl. Phys. B* **1020**, 117144 (2025).
- [22] A. Iorio, Curved Spacetimes and Curved Graphene: a status report of the Weyl-symmetry approach, *Int. J. Mod. Phys. D* **4**, 1530013 (2015).
- [23] A.A. Saharian, T.A. Petrosyan, A.A. Hovhannisyan, Casimir Effect for Fermion Condensate in Conical Rings, *Universe* **7**, 73 (2021).
- [24] S. Bellucci, I. Brevik, A.A. Saharian, H.G. Sargsyan, The Casimir effect for fermionic currents in conical rings with applications to graphene ribbons, *Eur. Phys. J. C* **80**, 281 (2020).
- [25] A.A. Saharian, V.F. Manukyan, T.A. Petrosyan, Finite temperature fermionic charge and current densities in conical space with a circular edge, *Phys. Rev. D* **111**, 065006 (2025).
- [26] A.A. Saharian, T.A. Petrosyan, Casimir densities induced by a sphere in the hyperbolic vacuum of de Sitter spacetime, *Phys. Rev. D* **104**, 065017 (2021).
- [27] A.A. Saharian, T.A. Petrosyan, and V.S. Torosyan, Mean field squared and energy-momentum tensor for the hyperbolic vacuum in dS spacetime, *Ann. Phys.* **437**, 168728 (2022).

- [28] A.A. Saharian, T.A. Petrosyan, The Casimir densities for a sphere in the Milne Universe, *Symmetry* **12**, 619 (2020).
- [29] M. Bañados, C. Teitelboim, J. Zanelli, The black hole in three dimensional spacetime, *Phys. Rev. Lett.* **69**, 1849 (1992).
- [30] J.D. Brown, M. Henneaux, Central charges in the canonical realization of asymptotic symmetries: an example from three dimensional gravity, *Commun. Math. Phys.* **104**, 207 (1986).
- [31] S. Carlip, The (2+1)-Dimensional Black Hole, *Class. Quantum Grav.* **12**, 2853 (1995).
- [32] S. Carlip, What we don't know about BTZ black hole entropy, *Class. Quantum Grav.* **15**, 3609 (1998).
- [33] A. Strominger, Black hole entropy from near-horizon microstates, *J. High Energ. Phys.* **9802**, 009 (1998).
- [34] R. Emparan, A. M. Frassino, B. Way, Quantum BTZ black hole, *J. High Energ. Phys.* **2020**, 137 (2020).
- [35] A.A. Saharian, *The Generalized Abel-Plana Formula with Applications to Bessel Functions and Casimir Effect* (Yerevan State University Publishing House, Yerevan, 2008) (arXiv:0708.1187).
- [36] F.W. Olver et al., *NIST Handbook of Mathematical Functions* (Cambridge University Press, USA, 2010).
- [37] V.Kh. Kotanjyan, A.A. Saharian, M.R. Setare, Vacuum currents in partially compactified Rindler spacetime with an application to cylindrical black holes, *Nuclear Physics B* **980**, 115838 (2022).
- [38] *Handbook of Mathematical Functions*, edited by M. Abramowitz and I.A. Stegun (Dover, New York, 1972).
- [39] A.P. Prudnikov, Yu.A. Brychkov, O.I. Marichev, *Integrals and Series* (Gordon and Breach, New York, 1986), Vol. 2.